HHS Public Access

Author manuscript

Nat Cell Biol. Author manuscript; available in PMC 2009 June 01.

Published in final edited form as:

Nat Cell Biol. 2008 December ; 10(12): 1440–1446. doi:10.1038/ncb1803.

Regulation of the *Drosophila* Apoptosome through Feedback Inhibition

Peter J. Shapiro[1,+], **Hans H. Hsu**[1,+], **Heekyung Jung**[1,+], **Edith S. Robbins**[1], and **Hyung Don Ryoo**[1,*]

[1]Department of Cell Biology, New York University School of Medicine, 550 First Avenue, New York, NY 10016

Abstract

Apoptosis is induced by caspases, which are members of the cysteine protease family 1. Caspases are synthesized as inactive zymogens and initiator caspases first gain activity by associating with an oligomeric complex of their adaptor proteins, such as the apoptosome 2,3. Activated initiator caspases subsequently cleave and activate effector caspases. While such a proteolytic cascade would predict that a small number of active caspases could irreversibly amplify caspase activity and trigger apoptosis, many cells can maintain moderate levels of caspase activity to perform non-apoptotic roles in cellular differentiation, shape change and migration 4. Here we show that the *Drosophila* apoptosome engages in a feedback inhibitory loop, thereby moderating its activation level *in vivo*. Specifically, the adaptor protein Apaf-1 lowers the level of its associated initiator caspase, Dronc, without triggering apoptosis. Conversely, Dronc lowers Apaf-1 protein levels. This mutual suppression depends upon Dronc's catalytic site and a caspase cleavage site within Apaf-1. Moreover, the *Drosophila* Inhibitor of Apoptosis Protein 1 (Diap1) is required for this process. We speculate that this feedback inhibition allows cells to regulate the degree of caspase activation for apoptotic and non-apoptotic purposes.

The *Drosophila* apoptosome holoenzyme at its core contains two protein components; the initiator caspase Dronc and the *Drosophila* Apaf-1 homolog that is known as *apaf-1 related killer* (*ark*), *hac-1* or *d-apaf-1* 5 (henceforth referred to as Apaf-1). Their importance is evident from the fact that most apoptosis in this organism is abolished in mutants lacking these genes 6–12. While active *Drosophila* caspases can be generated *in vitro* simply with dNTPs, Dronc and Apaf-1 5,13, broadly overexpressing Apaf-1 in developing *Drosophila* tissues through the *engrailed* (*en*) or *armadillo* (*arm*) promoters did not cause massive apoptosis, despite a considerable level of endogenous Dronc normally expressed in these tissues (Figure 1A,D). The inability of Apaf-1 to trigger apoptosis correlated with the unexpected observation that Apaf-1 expressing cells had diminished Dronc protein levels (Figure 1A,B,D). The reduction of Dronc protein was not due to lower *dronc* mRNA levels as assessed by fluorescent in situ hybridization (Figure 1A",B"). Western blot analyses of

[*]Corresponding author: Hyung Don Ryoo, Tel: 212-263-7257, Fax: 917-992-2874.
[+]These authors contributed equally

Dronc also yielded similar results (Figure 1C,D). In healthy Schneider cells, the polyclonal anti-Dronc antibody detected primarily the proenzyme form of Dronc as judged by its molecular weight. When these cells were stressed by treatment with a high concentration of DMSO, the antibody readily detected a faster migrating band indicative of a processed Dronc species (Figure 1C). We also examined Dronc protein in larval extracts. When a control protein, GFP, was ubiquitously expressed through the *arm* promoter, we primarily detected the proenzyme form of Dronc as assessed through western blots. When we attempted to activate Dronc in these larval cells by overexpressing a stable and hyperactive Apaf-1 variant (*dark*^{V})14 under otherwise similar conditions, the levels of the proenzyme Dronc were reduced without generating a detectable amount of the processed Dronc band (Figure 1D). Conversely, we found higher Dronc levels in cells of *apaf-1* loss-of-function mosaic clones within imaginal discs (Figure 1E). These results establish that Apaf-1 suppresses Dronc protein levels *in vivo*.

We also found evidence for a converse relationship between Apaf-1 and Dronc, in which endogenous Dronc protein limits Apaf-1 protein accumulation. When *dronc* −/− mosaic clones were generated in discs misexpressing Apaf-1 with the *en* promoter, we were able to detect higher levels of Apaf-1 in many *dronc* −/− mosaic clones, as detected through a myc-tag associated with the Apaf-1 transgene (Supplementary Information 1). As Apaf-1 and Dronc have been established as binding partners for cell death execution, our observations reveal an unexpected relationship between Apaf-1 and Dronc proteins in mutually suppressing each other in living cells.

Since overexpression of Apaf-1 alone did not lead to apoptosis, we attempted to achieve apoptosome activation *in vivo* by co-expressing Apaf-1 and Dronc. These experiments were performed in eye imaginal discs using the eye-specific gene expression driver, *gmr-Gal4* (Figure 2). Apaf-1 overexpression through the *gmr* promoter neither induced significant levels of apoptosis in larval eye discs as could be detected through antibody labeling against anti-cleaved caspases, nor caused eye ablation in adults (Figure 2A,E'). Similarly, when high levels of Dronc were induced, no significant apoptosis could be detected in larval eye discs and did not cause an obvious eye ablation phenotype in adults (Figure 1B,F'). By contrast, Apaf-1 and Dronc co-expression caused massive apoptosis, as assessed by anti-cleaved caspase antibody labeling in eye imaginal discs and by the ablated head structure in adults (Figure 2C,G'). Moreover, this eye ablation phenotype was completely suppressed when Diap1 was co-expressed with the apoptosome components (Figure 2D).

Interestingly, discs co-expressing Apaf-1 and Dronc showed lower Apaf-1 immuno-labeling, compared to those eye discs in which Apaf-1 was overexpressed alone (Figure 2E"',G"'). The difference in Apaf-1 labeling was particularly prominent in the posterior end of eye discs, which contain mostly post-mitotic ommatidial cells. The effect of Dronc overexpression on Apaf-1 levels was also observed using a flip-out technology that generates mosaic clones expressing genes of choice through the *tubulin*-promoter (see Methods). As a control, we generated mosaic clones that expressed either Apaf-1 or Dronc alone and observed large mosaic clones with high and uniform levels of these proteins (Figure 2H,I). By contrast, when mosaic clones co-expressing Dronc and Apaf-1 were generated, which were marked by the absence of GFP, only a small number of cells survived

to form mosaic clones. But within the surviving cells, which were mostly in the posterior part of eye discs, significantly lower levels of Apaf-1 were detected (Figure 2J). This indicates that Dronc suppresses Apaf-1 and the efficiency of this suppression is particularly prominent in posterior eye discs, where post-mitotic cells showed enhanced resistance to Dronc and Apaf-1 induced apoptosis.

Since Apaf-1's primary role is to help Dronc activate its catalytic activity, we next determined whether Apaf-1 and Dronc's mutually repressive effects require Dronc function. Through immuno-labeling of wing imaginal discs, we first compared the effect of overexpressed Apaf-1 on the endogenous Dronc protein that is either derived from a wild type allele, or from a loss-of-function *dronc* allele (*dronc*^{L32}) that has a missense mutation in the CARD domain 12 (Figure 3A). Since homozygous *dronc*^{L32} −/− animals did not survive up to the 3rd instar larval stage in which our analysis was performed, we compared the wild type and L32 alleles when in trans over a *dronc* null allele, I29 12. Under these conditions, we found no detectable decrease in the levels of Dronc^{L32} protein in response to Apaf-1 overexpression (n=10), while all imaginal discs analyzed with the wild type *dronc* allele had its anti-Dronc immunolabeling reduced under an otherwise similar condition (n>50), suggesting that Dronc activity is required for its depletion (Figure 3B,C).

We also examined the capacity of an inactive Dronc to participate in this reciprocal regulation with Apaf-1 by co-expressing the two proteins in eye imaginal discs through the *gmr-Gal4* driver. When Apaf-1 levels were assessed through western blots on imaginal disc extracts expressing various combinations of Apaf-1 and Dronc, we found that co-expression of wild type Dronc led to an average of 15 fold reduction in the levels of the full-length myc-tagged Apaf-1 (n=3, p=0.00017, significant), as compared to those expressing Apaf-1 alone (Figure 3E). On the other hand, a catalytically inactive Dronc transgene, Dronc$^{C->A}$, did not significantly reduce myc-tagged Apaf-1 levels (n=3, p=0.16) (Figure 3D,E). To validate the western blot analysis, we performed an immunohistochemical analysis of imaginal discs expressing different combinations of Apaf-1 and Dronc. While co-expression of wild type Apaf-1 and Dronc yielded significantly lower levels of each protein than when each was expressed separately, this mutually repressive effect was not observed in a similar experiment with the Dronc$^{C->A}$ transgene (Figure 3F~H). Next, we tested if Dronc's effect on Apaf-1 is indirect, through the activity of effector caspases that become proteolytically active by Dronc. To determine this, we used the caspase inhibitor p35, which efficiently blocks effector caspases while not affecting Dronc 15,16. After analyzing 8 individual discs of each genotype labeled under identical conditions, we were able to detect significant reduction of myc-tagged Apaf-1 in response to Dronc co-expression. The added expression of p35 together with Dronc and Apaf-1 did not affect the levels of myc-tagged Apaf-1 protein, when compared with those without p35 (Supplementary Information 2). These results indicate that the mutually repressive nature of Dronc and Apaf-1 requires the catalytic activity of Dronc.

Abrams and colleagues have shown evidence that caspases cleave and destabilize Apaf-1 14. To test if this cleavage site within Apaf-1 is involved in the mutually suppressive relationship between Dronc and Apaf-1, we co-expressed an uncleavable Apaf-1 mutant construct generated by Abrams and colleagues, *dark*^{V}, together with Dronc in eye imaginal

discs (Figure 4). When the levels of myc-tagged Apaf-1 proteins were compared in the presence or absence of Dronc co-expression through western blots, we found that the wild type Apaf-1 protein was reduced approximately 10 fold with Dronc co-expression (n=3, p=0.00047, significant). By contrast, we did not see a statistically significant change in the levels of the cleavage resistant Apaf-1 (*dark*^{V}) protein in the presence or absence of Dronc misexpression (n=3, p=0.6686) (Figure 4B,C). Consistent with the western blot analysis, we were able to detect using whole mount immuno-labeling only low levels of Apaf-1 in control discs misexpressing wild type Apaf-1 (*dark*^{wt}) and Dronc (Figure 4D), while a significantly higher level of Apaf-1 was detected when the cleavage resistant Apaf-1 (*dark*^{V}) was co-expressed with Dronc under an otherwise identical condition (Figure 4E). Higher levels of the cleavage resistant Apaf-1 protein led to a dramatic reduction in overexpressed Dronc protein levels, demonstrating that this mutant Apaf-1 has shifted the balance between the two protein components of the apoptosome. In spite of their distinct effects on the relative protein levels of Apaf-1 and Dronc, the extent of eye ablation in adults expressing either the wild type or the cleavage resistant Apaf-1 protein appeared similar (Supplementary Information 3). We interpret that the cleavage-resistant Apaf-1 protein appears to change the equilibrium between Apaf-1 and Dronc through feedback inhibition, but not the steady state levels of active apoptosomes that these components generate. To make more active apoptosomes, we predict that further stabilization of both components might be required.

Since Apaf-1 levels in the above experiments were assessed through associated myc-tags at the C-terminus, we independently assessed Apaf-1 protein levels with constructs that had GFP tagged at their N-terminus. Specifically, we examined wild type and mutant Apaf-1 constructs with changes that either make them caspase cleavage resistant (Apaf-1^{V}) or that introduce a premature stop codon thereby mimicking the caspase cleaved product (Figure 4F). Transgenic *uas-GFP-apaf-1* flies, in which the wild type and mutant Apaf-1^{CC} transgenes were targeted to a defined genetic loci (51D) were generated using the phiC31 integrase system 17,18. When these transgenes were expressed in imaginal discs through the *en-Gal4* driver, we detected significantly less GFP-Apaf-1^{CC} protein when compared to the GFP-Apaf-1^{WT} protein (Figure 4G,H). Similarly, when these constructs were transfected in cultured Schneider cells, the cleavage resistant Apaf-1^{v} accumulated to the highest levels, while the Apaf^{CC} protein levels were the lowest among those tested (Figure 4I). When expressed in imaginal discs, the GFP-Apaf-1^{CC} expression did not generate any phenotypes that were associated with the wild type GFP-Apaf-1 expression: These included the ability to reduce endogenous Dronc levels when misexpressed (Figure 4G',H"), as well as the ability to trigger apoptosis when co-expressed with Dronc in the eye imaginal discs (Supplementary Information 4). Together, these data indicate that the absence of the C-terminal fragment prohibits Apaf-1 from accumulating to substantial levels to exert its pro-apoptotic activity.

The *Drosophila reaper*, *hid* and *grim* genes are potent inducers of apoptosis and also well-established activators of Dronc 16,19–22. The apparent difference between Diap1 antagonists and Apaf-1 in their ability to activate apoptosis prompted us to compare the effect of Apaf-1 and *hid* on Dronc protein levels. When Apaf-1 was overexpressed in mosaic

clones, these cells had lower anti-Dronc labeling (Figure 5A). To assess the effect of *hid*, we kept the *hid* expressing cells alive by co-expressing the effector caspase inhibitor *p35*, which does not affect Dronc function 16. In stark contrast to Apaf-1 expressing clones, those expressing *hid* and p35 showed enhanced anti-Dronc labeling, while *p35* alone did not (Figure 5B,D). Moreover, *hid* expression allowed Dronc and myc-tagged Apaf-1 to co-exist in cells when *hid, p35, apaf-1* were co-expressed (Figure 5C). These results indicate that *hid* acts as a potent pro-apoptotic molecule by allowing Apaf-1 and Dronc to cooperate in cells.

Since Diap1 is a major target of *hid's* pro-apoptotic function 22–25, we examined possible physical interactions between Diap1 and the apoptosome components (Supplementary Information 5). In GST pull downs, the wild type and the BIR1 mutant (6-3s allele24) GST-Diap1 proteins interacted with Dronc, while the Bir2 (23-4s allele24) mutant did not. This establishes that recombinant Diap1 protein specifically interacts with Dronc through Diap1's BIR2 domain. When GST-Apaf-1 protein was added together with recombinant Dronc and Diap1 proteins, we found that this GST-Apaf-1 formed a complex with ^{35}S-labeled Diap1 only in the presence of Dronc. Together, these results establish that Diap1 can form a complex together with Dronc and Apaf-1 in vitro (Supplementary Information 5C).

To examine the functional significance of Diap1 in regulating the apoptosome components, we took advantage of the *diap1$^{33\text{-}1s}$* allele, an ENU mutant allele lacking the C-terminal ubiqutin-ligase domain 26. We expressed Apaf-1 in the posterior compartments of wing imaginal discs that harbored a mixture of *diap1$^{33\text{-}1s}$ −/−* and *diap1+* mosaic clones. To keep the *diap1 −/−* clones alive in this tissue, we also broadly expressed in this compartment the effector caspase inhibitor p35. While overexpressed Apaf-1 readily reduced Dronc labeling in control cells of the *diap1+; p35+* genotype, neighboring clones of *diap1$^{33\text{-}1s}$−/−; p35+* cells were insensitive to Apaf-1 expression and did not show lower Dronc levels under otherwise identical conditions. Conversely, Apaf-1 protein detection in these cells was not affected by the presence of Dronc (Figure 5E,F). This indicates that Diap1's RING activity prevents Apaf-1 and Dronc from accumulating together in living cells.

A few distinct models by which Diap1 ubiquitylates Dronc have been proposed: First, Clem and colleagues have reported that Diap1 ubiquitylates mainly the processed, and therefore, active Dronc for ubiquitin-mediated degradation in cultured Schneider cells 27. On the other hand, Meier and colleagues have reported that Diap1 primarily ubiquitylates the full length, and therefore unprocessed Dronc for its inhibition, but this does not lead to a proteasome dependent degradation 26. Furthermore, Ciechanover and colleagues have shown that Diap1 can add ubiquitin to its substrates in a distinct configuration that is not recognized by the proteasome pathway 28. In accounting for our observations, the Clem model may predict that Diap1 triggers the degradation of processed Dronc, while an as yet unknown mechanism helps degrade the caspase cleaved form of Apaf-1. On the other hand, the Meier and Ciechanover models, together with our findings that Diap1 can form a complex together with Apaf-1 and Dronc, supports a speculative model, where Diap1 adds polyubiquitin chains for proteasome-degradation only to the active apoptosome complex, but not to Dronc monomers. These and other possible models remain to be validated *in vivo*.

In conclusion, we believe that the observed relationship between Apaf-1, Dronc and Diap1 can be most simply interpreted through the following model (Figure 5G): In many *Drosophila* cell types that normally express Apaf-1 and Dronc, low levels of active apoptosome complexes are constantly generated and are quickly subjected to feedback inhibition through degradation, instead of exponentially amplifying caspase activity and triggering unnecessary cell death. An early event in this inhibition is the proteolytic cleavage of Apaf-1 by Dronc, which destabilizes the entire Apaf-1 protein. Since the Diap1 RING domain-deleted mutant abolishes the negative relationship between Dronc and Apaf-1 and triggers apoptosis, Diap1 likely acts as a ubiquitin-ligase that promotes the degradation of the active apoptosome. Our observation that Apaf-1 undergoes feedback inhibition contradicts a popular view that the apoptosome is constitutively active and is not regulated in *Drosophila* 29. Moreover, because Diap1 keeps apoptosome levels in check, our model explains why nearly all apoptosis in *Drosophila* requires the expression of the Diap1 antagonists, *reaper*, *hid* and *grim*.

Methods

Fly strains

Genes were overexpressed in *Drosophila* imaginal discs through the standard Gal4/UAS system 30. The specific genotypes for individual experiments are labeled in the figure legends. *uas-dark* 14, *uas-dronc*, *uas-dronc*$^{C->A}$ 16, *uas-hid* and *uas-p35* 20 lines were as described previously. To co-express Dronc and Apaf-1, we recombined *uas-dronc* and *uas-apaf-1* onto the 3rd chromosome. These transgenes were misexpressed through *en-Gal4*, *gmr-Gal4*, *arm-Gal4* or *tubulin>FRT>y+*, *GFP>FRT>Gal4* (abbreviated in the text as *tub>GFP>Gal4*) drivers. Mosaic loss-of-function clones and flip out clones were induced through the standard FLP/FRT system 31,32. The loss of function mutant strains, *apaf-1*^{N28} (originally described as *dark*^{N28}), *dronc*^{L32}, *dronc*^{I29} and *diap1*$^{33\text{-}1s}$ had been described previously 9,12,26. To analyze GFP-Apaf-1, we fused EGFP to the N-terminal side of either the full length Apaf-1 coding sequence, or a truncated Apaf-1 that has a stop codon engineered in place of a.a. 1292 (referred to as Apaf-1^{CC}), subcloned into pUAST-attB and targeted to the 51D locus for insertion through the phiC31-integrase system 17,18.

Immunohistochemistry and western blots

All fluorescent images were obtained with a Zeiss LSM510 confocal microscope, using 20x or 40x objective lenses. Following are the antibodies used for this study: Guinea Pig anti-Dronc raised against the full length recombinant protein 33, monoclonal 9E10 (DSHB, Univ. Iowa) and rabbit anti-myc (Santa Cruz) for myc-tag detection, Rabbit anti-cleaved caspase (Cell Signaling Technologies), Guinea Pig anti-Hsc3 34 and Rabbit anti-GFP (Molecular Probes). For fluorescent in situ hybridization, we used the Perkin Elmer TSA-Cy5 kit. For anti-Dronc western blots in Figure 1, Schneider cells (Figure 1C) or whole larvae (Figure 1D) were ground in 5% SDS-loading buffer before analysis. For anti-myc western blots in Figure 3 and 4, we loaded into each lanes extracts prepared from forty eye-antennal imaginal discs isolated from late 3rd-instar larvae. For quantification of western bands and whole-mount immuno-labelings, we used image J software (http://rsbweb.nih.gov/ij). The intensity of the band of interest was normalized with either an anti-

Hsc3 band (Figure 3) or a nonspecific 120kDa band present in the same lane (Figure 4B). The statistical significance was assessed through t-test (two-tailed). To assess GFP-Apaf-1 levels in Schneider cell cultures, we transfected UAS-GFP-Apaf-1 constructs together with an actin-Gal4 plasmid.

Scanning Electron Microscopy

Standard procedures were followed for sample preparation, including fixation in 2% glutaraldehyde, dehydration and drying in HMDS solvent. Gold-Paladium was used to coat adult flies and images were taken at a 180x magnification.

GST pull down

The Diap1 proteins used in this study were full length 35. The mutant Diap1 proteins were derived from previously reported alleles 24. The Dronc protein used in the in vitro binding assay was near full length, catalytically dead and has been described previously 33. The recombinant Apaf-1 protein was from its natural initiation Met to amino acid 729, and thus lacked the C-terminal WD repeats. Diap1 was labeled with ^{35}S-Methionine using the Roche TNT kit.

Supplementary Material

Refer to Web version on PubMed Central for supplementary material.

Acknowledgements

We thank John Abrams, Andreas Bergmann, George Jackson, Pascal Meier for fly stocks, David Sabatini for making available the Scanning Electron Microscope, Milton Adesnik, Ramanuj Dasgupta, Zehra Ordulu, David Sabatini, Greg Suh and Jessica Treisman for advice and comments on the manuscript. P. J. S. is supported by an NIH pre-doctoral training grant 5T32GM007239-32. H.D.R. is a Special Fellow of the Leukemia-Lymphoma Society, a Basil O'Conner Scholar of the March of Dimes Foundation and an Ellison Medical Foundation New Scholar. This work was supported by a grant from the National Institutes of Health (1RO1GM079425) to H.D.R.

References

1. Thornberry NA, Lazebnik Y. Caspases: enemies within. Science. 1998; 281:1312–1316. [PubMed: 9721091]
2. Zou H, Li Y, Liu X, Wang X. An APAF-1 cytochrome c multimeric complex is a functional apoptosome that activates procaspase-9. J. Biol. Chem. 1999; 274:11549–11556. [PubMed: 10206961]
3. Rodriguez J, Lazebnik Y. Caspase-9 and Apaf-1 form an active holoenzyme. Genes Dev. 1999; 13:3179–3184. [PubMed: 10617566]
4. Kuranaga E, Miura M. Nonapoptotic functions of caspases: caspases as regulatory molecules for immunity and cell-fate determination. Trends Cell Biol. 17:135–144. [PubMed: 17275304]
5. Yu X, Wang L, Acehan D, Wang X, Akey CW. Three-dimensional structure of a double apoptosome formed by the Drosophila Apaf-1 related killer. J. Mol. Biol. 2006; 355:577–589. [PubMed: 16310803]
6. Rodriguez A, Oliver H, Zou H, Chen P, Wang X, Abrams JM. Dark is a Drosophila homologue of Apaf-1/CED-4 and functions in an evolutionarily conserved death pathway. Nat. Cell Biol. 1999; 1:272–279. [PubMed: 10559939]
7. Zhou L, Song Z, Tittel J, Steller H. HAC-1, a Drosophila homolog of APAF-1 and CED-4 functions in developmental and radiation-induced apoptosis. Mol. Cell. 1999; 4:745–755. [PubMed: 10619022]

8. Kanuka H, Sawamoto K, Inohara N, Matsuno K, Okano H, Miura M. Control of the cell death pathway by Dapaf-1, a Drosophila Apaf-1/CED-4-related caspase activator. Mol. Cell. 1999; 4:757–769. [PubMed: 10619023]

9. Srivastava M, Scherr H, Lackey M, Xu D, Chen Z, Lu J, Bergmann A. ARK, the Apaf-1 related killer in Drosophila, requires diverse domains for its apoptotic activity. Cell Death Differ. 2006; 14:92–102. [PubMed: 16645639]

10. Chew SK, Akdemisr F, Chen P, Lu WJ, Mills K, Daish T, Kumar S, Rodriguez A, Abrams JM. The apical caspase dronc governs programmed and unprogrammed cell death in Drosophila. Dev. Cell. 2004; 7:897–907. [PubMed: 15572131]

11. Daish TJ, Mills K, Kumar S. Drosophila caspase DRONC is required for specific developmental cell death pathways and stress-induced apoptosis. Dev. Cell. 2004; 7:909–915. [PubMed: 15572132]

12. Xu D, Li Y, Arcaro M, Lackey M, Bergmann A. The CARD-carrying caspase Dronc is essential for most, but not all, developmental cell death in Drosophila. Development. 2005; 132:2125–2134. [PubMed: 15800001]

13. Yan N, Huh JR, Schirf V, Demeler B, Hay BA, Shi Y. Structure and activation mechanism of the Drosophila initiator caspase Dronc. J. Biol. Chem. 2006; 281:8667–8674. [PubMed: 16446367]

14. Akdemir F, Farkas R, Chen P, Juhasz G, Medved'ova L, Sass M, Wang L, Wang X, Chittaranjan S, Gorski SM, Rodriguez A, Abrams JM. Autophagy occurs upstream or parallel to the apoptosome during histolytic cell death. Development. 2006; 113:1457–1465. [PubMed: 16540507]

15. Clem RJ, Fechheimer M, Miller K. Prevention of apoptosis by a baculovirus gene during infection of insect cells. Science. 1991; 254:1388–1390. [PubMed: 1962198]

16. Meier P, Silke J, Leevers SJ, Evan GI. The Drosophila caspase DRONC is regulated by DIAP1. EMBO J. 2000; 19:598–611. [PubMed: 10675329]

17. Groth AC, Fish M, Nusse R, Calos MP. Construction of transgenic Drosophila by using the site-specific integrase from phage phiC31. Genetics. 2004; 166:1775–1782. [PubMed: 15126397]

18. Bischof J, Maeda RK, Hediger M, Karch F, Basler K. An optimized transgenesis system for Drosophila using germ-line-specific phiC31 integrases. Proc. Natl. Acad. Sci. U.S.A. 2007; 104:3312–3317. [PubMed: 17360644]

19. White K, Grether ME, Abrams JM, Young L, Farrell K, Steller H. Genetic control of programmed cell death in Drosophila. Science. 1994; 264:677–683. [PubMed: 8171319]

20. Grether ME, Abrams JM, Agapite J, White K, Steller H. The head involution defective gene of Drosophila melanogaster functions in programmed cell death. Genes Dev. 1995; 9:1694–1708. [PubMed: 7622034]

21. Chen P, Nordstrom W, Gish B, Abrams JM. grim, a novel cell death gene in Drosophila. Genes Dev. 1996; 10:1773–1782. [PubMed: 8698237]

22. Steller H. Regulation of apoptosis in Drosophila. Cell Death Differ. 2008; 15:1132–1138. [PubMed: 18437164]

23. Wang SL, Hawkins CJ, Yoo SJ, Muller HA, Hay BA. The Drosophila caspase inhibitor DIAP1 is essential for cell survival and is negatively regulated by HID. Cell. 1999; 98:453–463. [PubMed: 10481910]

24. Goyal L, McCall K, Agapite J, Hartwieg E, Steller H. Induction of apoptosis by Drosophila reaper, hid and grim through inhibition of IAP function. EMBO. J. 2000; 19:589–597. [PubMed: 10675328]

25. Lisi S, Mazzon I, White K. Diverse domains of THREAD/DIAP1 are required to inhibit apoptosis induced by REAPER and HID in Drosophila. Genetics. 2000; 154:669–678. [PubMed: 10655220]

26. Wilson R, Goyal L, Ditzel M, Zachariou A, Baker DA, Agapite J, Steller H, Meier P. The DIAP1 RING finger mediates ubiquitination of Dronc and is indispensable for regulating apoptosis. Nat. Cell Biol. 2002; 4:445–450. [PubMed: 12021771]

27. Muro I, Hay BA, Clem RJ. The Drosophila DIAP1 protein is required to prevent accumulation of a continuously generated, processed form of the apical caspase DRONC. J. Biol. Chem. 2002; 277:49644–49650. [PubMed: 12397080]

28. Herman-Bachinsky Y, Ryoo HD, Ciechanover A, Gonen H. Regulation of the Drosophila ubiquitin ligase DIAP1 is mediated via several distinct ubiquitin system pathways. Cell Death Differ. 2007; 14:861–871. [PubMed: 17205079]

29. Kornbluth S, White K. Apoptosis in Drosophila: neither fish nor fowl (nor man nor worm). J. Cell Sci. 2005; 118:1779–1787. [PubMed: 15860727]

30. Brand AH, Perrimon N. Targeted gene expression as a means of altering cell fates and generating dominant phenotypes. Development. 1993; 118:401–415. [PubMed: 8223268]

31. Golic KG, Lindquist S. The FLP recombinase of yeast catalyzes site-specific recombination in the Drosophila genome. Cell. 1989; 59:499–509. [PubMed: 2509077]

32. Struhl G, Basler K. Organizing activity of wingless protein in Drosophila. Cell. 1993; 72:527–540. [PubMed: 8440019]

33. Ryoo HD, Ryoo HD, Gorenc T, Steller H. Apoptotic cells can induce compensatory cell proliferation through the JNK and the Wingless signaling pathways. Dev. Cell. 2004; 7:491–501. [PubMed: 15469838]

34. Ryoo HD, Domingos PM, Kang MJ, Steller H. Unfolded Protein Response in a Drosophila Model for Retinal Degeneration. EMBO J. 2007; 26:242–252. [PubMed: 17170705]

35. Ryoo HD, Bergmann A, Gonen H, Ciechanover A, Steller H. Regulation of Drosophila IAP1 degradation and apoptosis by reaper and ubcD1. Nat. Cell. Biol. 2002; 4:432–438. [PubMed: 12021769]

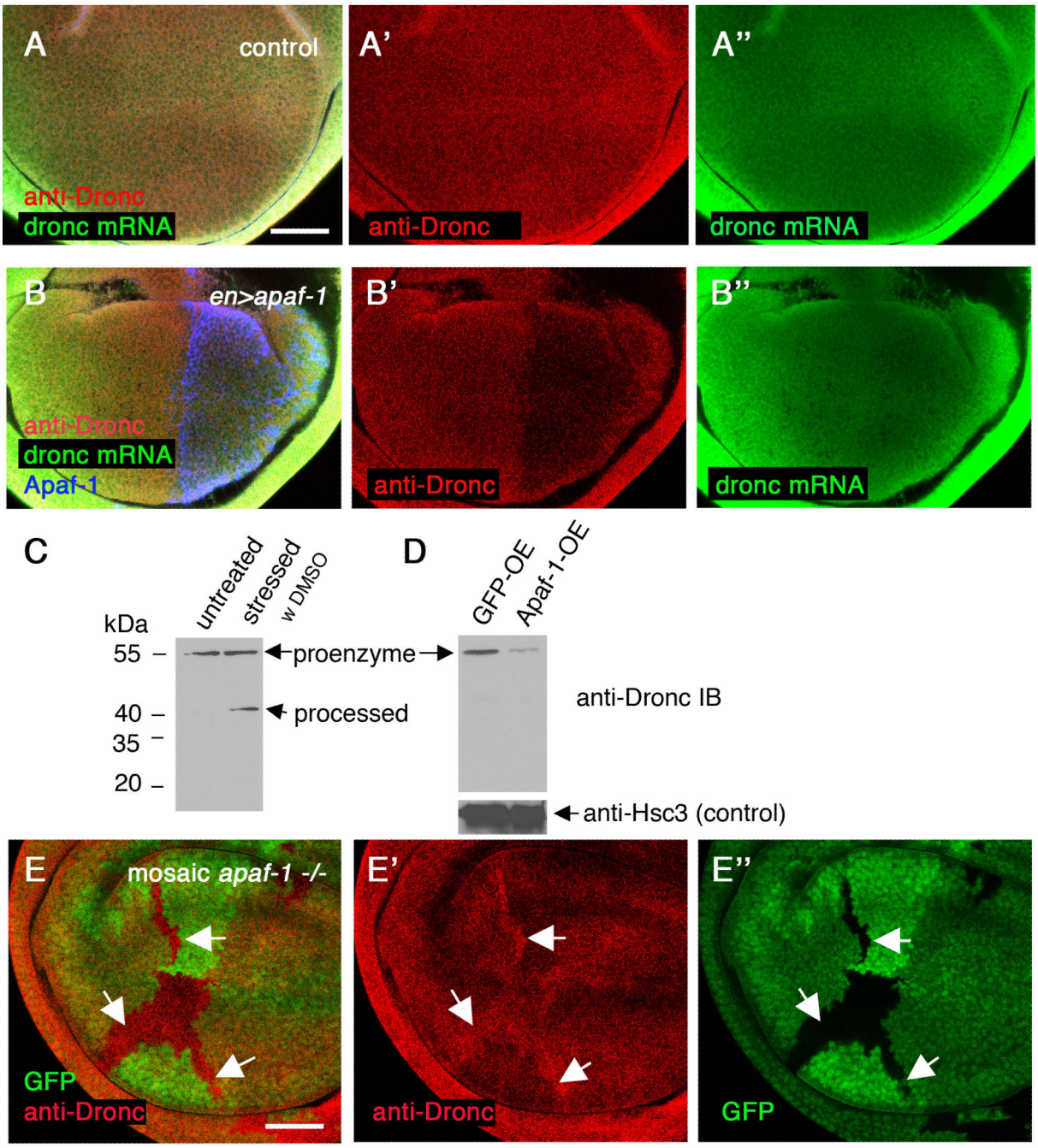

Figure 1. Apaf-1 lowers Dronc protein levels in *Drosophila* tissues

(A,B) anti-Dronc antibody labeling (red) and *dronc* mRNA in situ hybridization (green) in control wing imaginal discs (A), or those that were expressing Apaf-1 (B). Apaf-1 protein was detected through a C-terminally fused myc-tag (blue). Single channels of Dronc protein and mRNA are shown in (A',A",B',B"). (C) Schneider cell extracts immunoblotted with anti-Dronc antibody. A control cell extract showed primarily a 55kDa band corresponding to the full-length proenzyme (left lane), while 1% DMSO treatment for 1 hour prompted the emergence of a 40kDa species indicative of processed Dronc. (D) Extracts of larvae

expressing either GFP (left lane) or a stable form of Apaf-1, *dark*^{V} (right lane) were probed with anti-Dronc antibody. GFP and Apaf-1 were expressed ubiquitously through the *arm-Gal4* driver. The lower gel shows the same extracts immunoblotted with anti-Hsc3 as a control. (E) Anti-Dronc antibody labeling (red) in *apaf-1*^{N28} *−/−* mosaic clones (marked by the absence of GFP). Loss of *apaf-1* correlates with enhanced anti-Dronc labeling (white arrows). The scale bars represent 25 μm. Genotypes: (A) *en-Gal4/+*. (B) *en-Gal4/+; uas-apaf-1/+*. (D) (left lane) *arm-Gal4/ uas-GFP*. (right lane) *arm-Gal4/ uas-apaf-1*. (E) *hs-flp; FRT42, apaf-1*^{N28}*/ FRT42, ubi-GFP*.

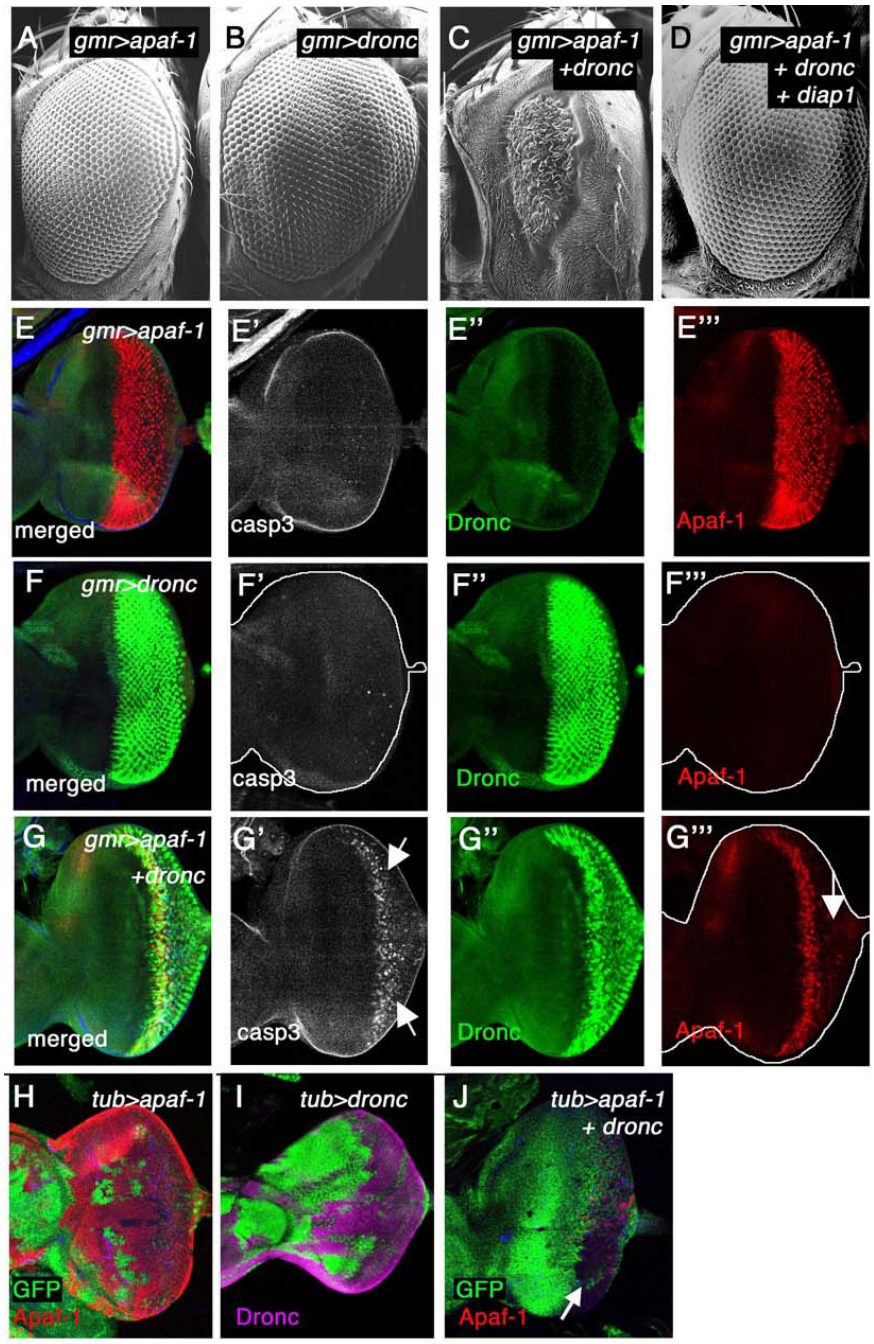

Figure 2. Overexpression of Apaf-1 and Dronc in eye imaginal discs

External adult eye (A–D) and larval eye imaginal discs (E–G) expressing either Apaf-1 alone (A,E), Dronc alone (B,F) co-expressing Apaf-1 and Dronc (C,G) through an eye-specific driver, *gmr-Gal4*. Co-expression of Apaf-1 and Dronc leads to adult eye ablation (C), while Diap1 expression rescues this phenotype (D). In all eye imaginal disc panels, Apaf-1 overexpression is detected through an associated myc-tag (red) and Dronc protein is detected through anti-Dronc antibody (green). Apoptosis was measured in (E',F',G') through anti-cleaved caspase-3 labeling (white, pointed with arrows in G'). Co-expression of

Dronc with Apaf-1 diminishes Apaf-1 labeling, particularly in posterior imaginal discs (arrow in G"'). (H–J) Expression of Apaf-1 alone (red) (H), Dronc alone (magenta) (I), or co-expression of Apaf-1 and Dronc (J) in mosaic clones (marked by the absence of GFP), through the flip-out Gal4/UAS technology. (J) Mosaic clones co-expressing Dronc and Apaf-1 survive in the posterior region of eye discs (arrow) and shows diminished levels of Apaf-1 labeling (red). The scale bar in (A) represents 100μm. The scale bar in (E) represents 50 μm. Genotype: (A,E) *GMR-Gal4/+; uas-apaf-1/+*. (B,F) *GMR-Gal4/+; uas-dronc/+*. (C,G) *GMR-Gal4/+; uas-dronc, uas-apaf-1/+*. (H) *ey-flp; tub>GFP>Gal4/uas-apaf-1*. (I) *ey-flp; tub>GFP>Gal4/uas-dronc*. (J) *ey-flp; tub>GFP>Gal4/ uas-apaf-1, uas-dronc*.

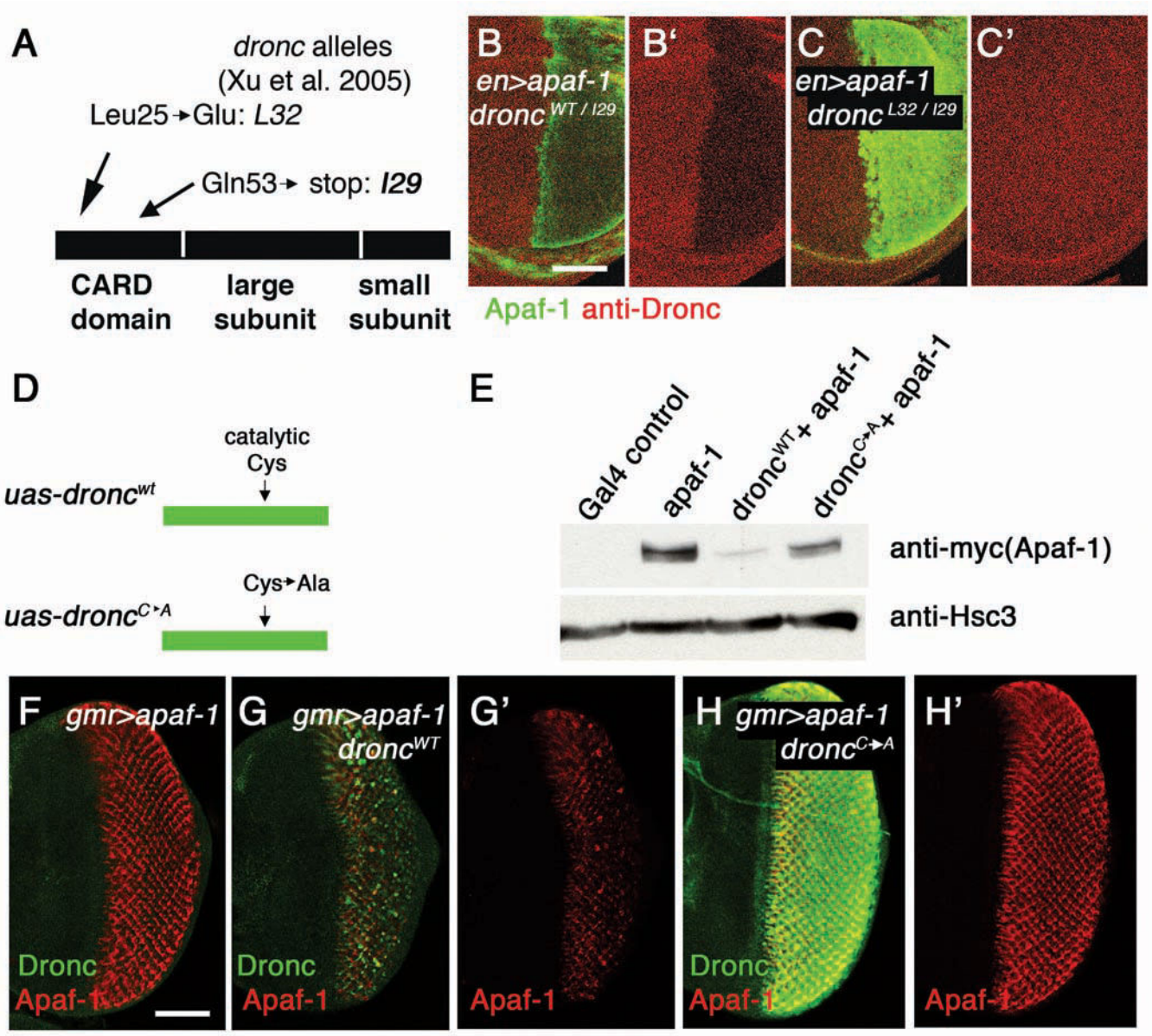

Figure 3. The mutually negative relationship between Dronc and Apaf-1 requires Dronc function

(A) A schematic diagram of the Dronc coding sequence and the nature of the *dronc* mutant alleles 12 used in this study. *dronc*^{I29} is a null allele and not detectable through immunolabeling. (B,C) Apaf-1 was expressed (green) in the posterior compartments of wing discs and its effects on either the wild type Dronc (B) or Dronc^{L32} mutant (C) were compared through anti-Dronc labeling (red). These *dronc* alleles were in trans over the null allele, *dronc*^{I29}. Under these conditions, misexpressed Apaf-1 effectively lowered the wild type Dronc protein, while it failed to suppress the levels of Dronc^{L32}. (D–H) The catalytic site of Dronc is required for the mutually negative regulation between Dronc and Apaf-1. (D) A schematic diagram of transgenic Dronc constructs misexpressed in eye imaginal discs. (E) A western blot of eye imaginal disc extracts overexexpressing the indicated genes. The genotypes were: (lane 1) *gmr-gal4*. (lane 2) *gmr-gal4/+; uas-apaf-1*. (lane 3) *gmr-Gal4/+;*

uas-dronc^{WT}, *uas-apaf-1*. (lane 4) *gmr-Gal4/+; uas-dronc*$^{C->A}$, *uas-apaf-1*. (F–H) Representative images of eye imaginal discs expressing Apaf-1 alone (F) or together with Dronc (G,H). Anti-Dronc antibody is labeled in (green) and Apaf-1 is detected through its myc-tag in (red). (G',H') Anti-Apaf-1 single channel of discs shown in (G,H). While both Apaf-1 and Dronc levels are low when wild type proteins were co-expressed through the *gmr*-promoter (G), significantly higher levels of Dronc and Apaf-1 were detected in discs expressing the catalytically inactive Dronc, Dronc$^{C->A}$ (H). The scale bars in (B,F) represent 50 μm. Genotype: (B) *en-Gal4/+; uas-apaf-1, dronc*^{I29}/+. (C) *en-Gal4/+; uas-apaf-1, dronc*^{I29}/ *dronc*^{L32}. (F) *gmr-gal4/+;uas-apaf-1/+*. (G) *gmr-gal4/+; uas-apaf-1, uas-dronc*. (H) *gmr-gal4/+; uas-apaf-1, uas-dronc*$^{C->A}$.

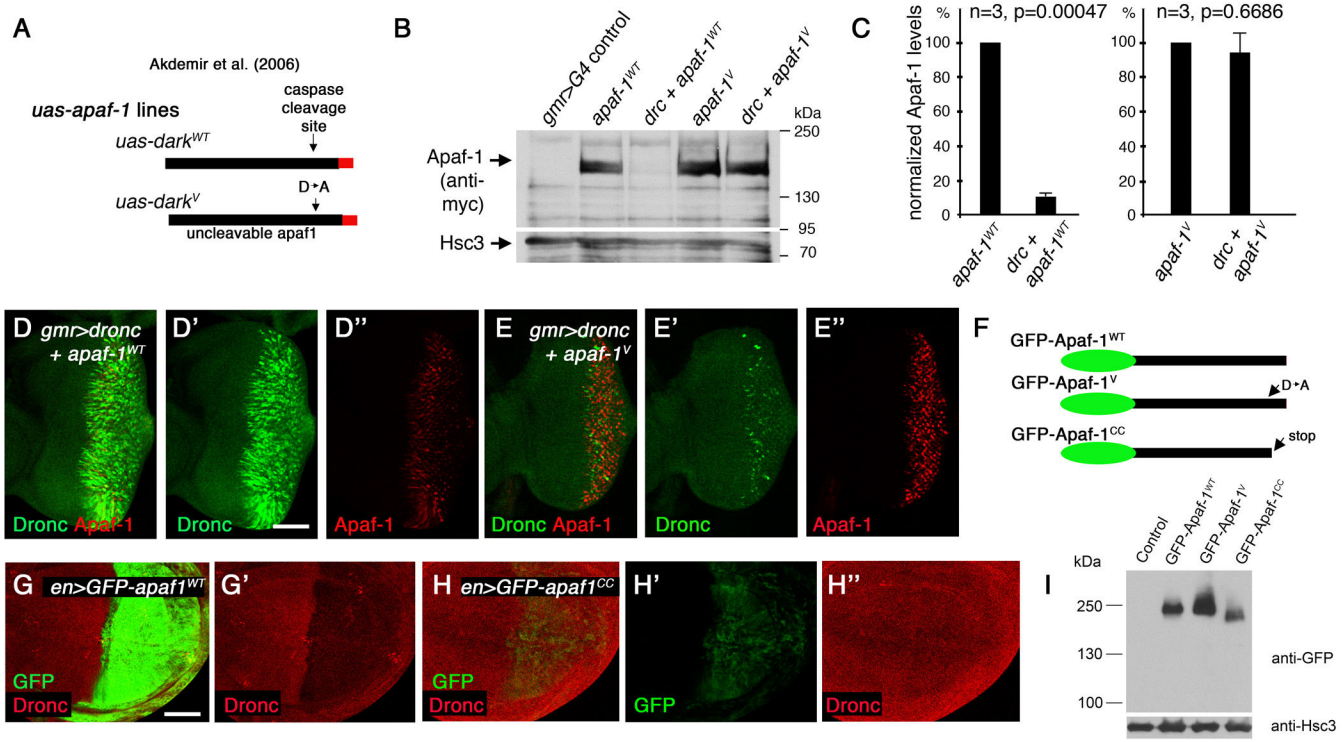

Figure 4. Dronc cleaves Apaf-1 through a caspase cleavage site

(A) A schematic diagram of mutant and wild type Apaf-1 overexpression constructs used in (B–E). The transgenic Apaf-1 constructs have C-terminally tagged myc-epitopes (red), previously described as *uas-dark* lines 28. (B) A representative western blot of eye imaginal disc extracts misexpressing the indicated combinations of Apaf-1 and Dronc (drc) transgenes through the *gmr-Gal4* driver. The upper gel shows bands corresponding to myc-tagged Apaf-1, while the lower gel shows Hsc3 bands as a loading control. (C) Comparison of the normalized Apaf-1 band intensity in the presence or absence of Dronc co-expression (average of n=3), with the value from Apaf-1-only expressing extracts set at 100%. The left graph compares the relative Apaf-1^{WT} intensity, while the right graph compares the levels of Apaf-1^{V}. Error bars indicate ±SEM. (D,E) Representative eye discs co-expressing indicated combinations of Dronc and Apaf-1 alleles through the *gmr-Gal4* driver. Anti-Dronc labeling is in (green), while anti-myc labeling is in (red). Individual channels are shown in (D',D", E', E"). (F) A schematic diagram of GFP-Apaf-1 constructs used in (G–I). GFP-Apaf-1^{V} has the putative caspase cleavage site disrupted, while GFP-Apaf-1^{CC} mimics a caspase cleaved product. (G) A wing disc expressing GFP-Apaf-1^{WT} (green) through the *en-Gal4* driver. Anti-Dronc labeling (red) was reduced in response to GFP-Apaf-1^{WT}. (H) GFP-Apaf-1^{CC} expression using an otherwise identical condition generated weaker GFP fluorescence and did not reduce anti-Dronc labeling. (G',G", H', H") Single channels of GFP and anti-Dronc respectively. The scale bars in (D,G) represent 50μm. (I) GFP-Apaf-1 proteins expressed in Schneider cells were probed with anti-GFP antibody (upper gel) and anti-Hsc3 for loading control (lower gel). Lane 1: Mock transfected control. Lane 2: GFP-Apaf-1^{WT}. Lane 3: GFP-Apaf-1^{V}. Lane 4: GFP-Apaf-1^{CC}. Genotypes: (D) *gmr-Gal4/+; uas-dronc, uas-*

apaf-1^{WT}/+. (E) *gmr-Gal4/+; uas-dronc, uas-apaf-1*^{V}/+. (G) *en-gal4/ uas-GFP-apaf-1*^{WT}. (H) *en-gal4/ uas-GFP-apaf-1*^{CC}.

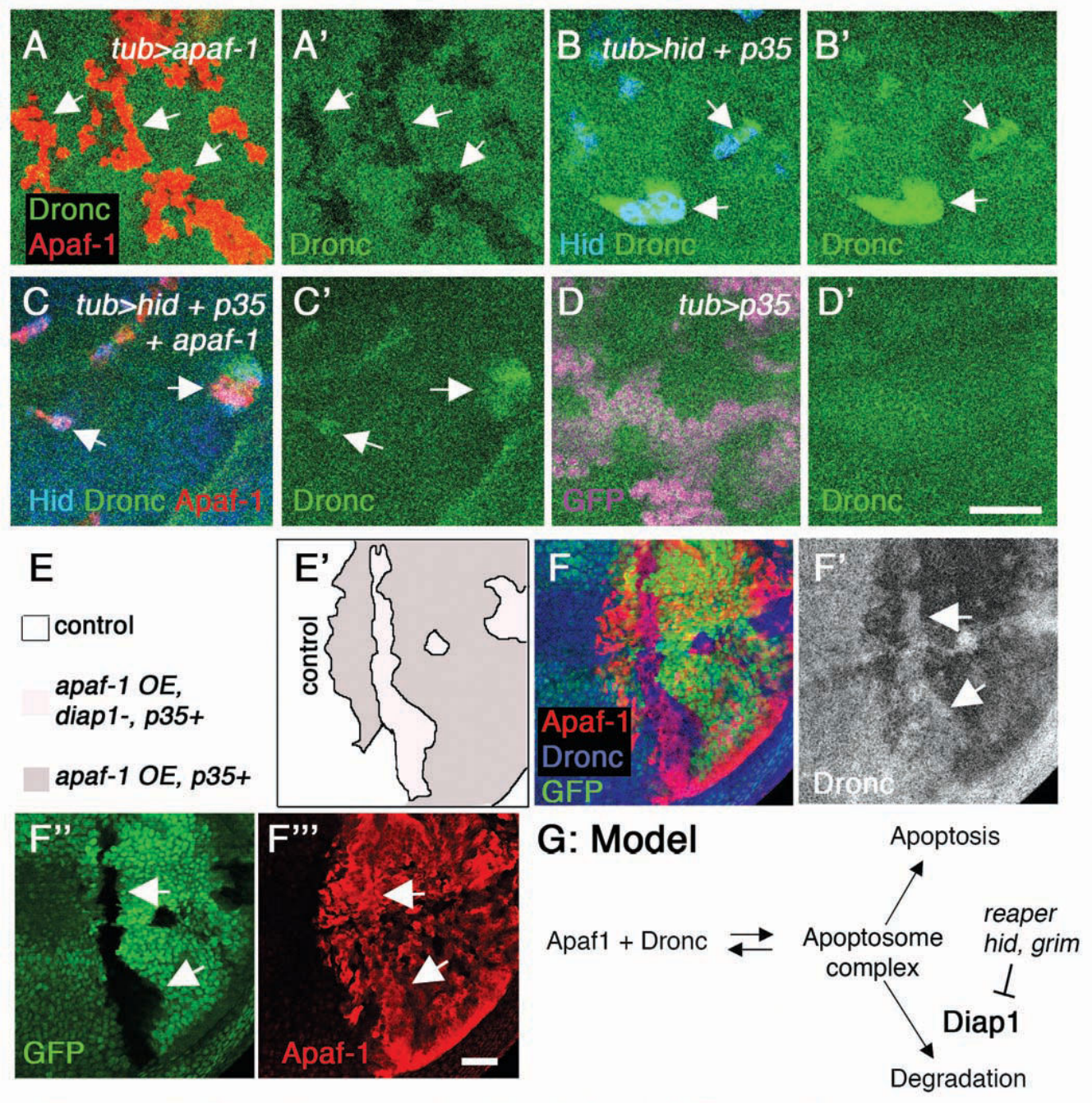

Figure 5. Diap1 prevents Apaf-1 and Dronc from accumulating together in cells

(A–D) Wing imaginal discs with mosaic clones overexpressing Apaf-1 (A), Hid and p35 (B), Hid, p35 and Apaf-1 (C), or p35 alone (D). Apaf-1 is detected through its C-terminal myc-tag (red), while Dronc (green) and Hid (blue) proteins were detected through polyclonal antibodies against them. (A) Apaf-1 overexpressing clones reduced Dronc labeling. (B) Hid and p35 co-expressing clones had enhanced Dronc labeling. (C) When Hid, p35 and Apaf-1 were co-expressed, Apaf-1 was detected together enhanced Dronc in these cells. (D) As a control, mosaic clones expressing p35 alone were generated (marked by

the absence of GFP in magenta), which had no effect on endogenous Dronc labeling. (E–G) Diap1 is required for the mutually suppressive activities between Apaf-1 and Dronc. (E,E') A schematic diagram of the genotypes of mosaic clones generated in the wing imaginal disc shown in (F). (F) A merged image that labels overexpressed Apaf-1 (red) and endogenous Dronc (blue). *diap1* −/− cells are marked by the absence of GFP (green) and pointed with white arrows. These cells were kept alive by expressing the effector caspase inhibitor p35 throughout the experimental domain. Single channel image of anti-Dronc (white) (F'), GFP (F") and overexpressed Apaf-1 (F"') are shown. (G) Model. Apaf-1 and Dronc associate with each other to form an oligomeric apoptosome complex. In living cells, the activity of Diap1 directs it to a degradation pathway. In response to death signals, Diap1 antagonists *reaper*, *hid* and *grim* are induced, which suppresses the apoptosome instability, thereby allowing the execution of apoptosis. The scale bar in (D') applies to (A–D), while the one in (F"') is for all panels of (F), representing 25 μm. Genotypes: (A) *hs-flp/+; tub>GFP>Gal4/ uas-apaf-1*. (B) *hs-flp/ uas-hid; uas-p35/+; tub>GFP>Gal4/+*. (C) *hs-flp/ uas-hid; uas-p35/+; uas-apaf-1/tub>GFP>Gal4*. (D) *hs-flp/+; uas-p35/+; tub>GFP>Gal4/+*. (E,F) *en-Gal4/ uas-flp, uas-p35; diap*$^{133\text{-}1s}$*,FRT80, uas-apaf-1/ ubi-GFP,FRT80*.